nature nanotechnology

LETTERS

PUBLISHED ONLINE: 25 MAY 2015 | DOI: 10.1038/NNANO.2015.97

Single-molecule diodes with high rectification ratios through environmental control

Brian Capozzi[1], Jianlong Xia[2], Olgun Adak[1], Emma J. Dell[2], Zhen-Fei Liu[3], Jeffrey C. Taylor[1], Jeffrey B. Neaton[3,4]*, Luis M. Campos[2]* and Latha Venkataraman[1,2]*

Molecular electronics aims to miniaturize electronic devices by using subnanometre-scale active components[1–3]. A single-molecule diode, a circuit element that directs current flow[4], was first proposed more than 40 years ago[5] and consisted of an asymmetric molecule comprising a donor–bridge–acceptor architecture to mimic a semiconductor p–n junction. Several single-molecule diodes have since been realized in junctions featuring asymmetric molecular backbones[6–8], molecule–electrode linkers[9] or electrode materials[10]. Despite these advances, molecular diodes have had limited potential for applications due to their low conductance, low rectification ratios, extreme sensitivity to the junction structure and high operating voltages[7–9,11,12]. Here, we demonstrate a powerful approach to induce current rectification in symmetric single-molecule junctions using two electrodes of the same metal, but breaking symmetry by exposing considerably different electrode areas to an ionic solution. This allows us to control the junction's electrostatic environment in an asymmetric fashion by simply changing the bias polarity. With this method, we reliably and reproducibly achieve rectification ratios in excess of 200 at voltages as low as 370 mV using a symmetric oligomer of thiophene-1,1-dioxide[13,14]. By taking advantage of the changes in the junction environment induced by the presence of an ionic solution, this method provides a general route for tuning nonlinear nanoscale device phenomena, which could potentially be applied in systems beyond single-molecule junctions.

In this Letter we use the scanning tunnelling microscope-based break junction technique[15] (STM-BJ) to rapidly and reproducibly measure the conductance ($G = I/V$) and current–voltage (I–V) characteristics of thousands of single-molecule junctions (see Methods and Supplementary Fig. 1). Using this technique, we demonstrate rectification in single-molecule junctions by carrying out measurements in propylene carbonate (PC), a polar solvent. We use an STM tip insulated with Apiezon wax[16] to reduce its area to ~1 μm^2 and a gold substrate with an area greater than 1 cm^2 (Fig. 1a). The insulation on the tip serves to reduce any background capacitive and Faradaic electrochemical currents stemming from the electrolyte, but, more importantly, it gives us control of the electrostatic environment around the tip and substrate.

We first demonstrate exceptionally high and statistically reproducible single-molecule junction rectification in an oligomer consisting of four thiophene-1,1-dioxide units flanked by two gold-binding methyl-sulphide-bearing thiophenes[13] (TDO4, Fig. 1a). Sample conductance versus displacement traces for TDO4 measured in PC are shown in the inset to Fig. 1b. Under the conditions described above, there is a significant difference in the single-molecule junction conductance measurements when performed at +180 mV or −180 mV (tip relative to substrate). When thousands of conductance traces are compiled, without data selection, into one-dimensional log-binned conductance histograms (Fig. 1b), it is clear that the conductance measured at −180 mV exceeds that measured at +180 mV by a factor of 3.25. This is a significant difference for such a low-bias measurement. This bias polarity-dependent conductance is not observed when TDO4 is measured in a nonpolar and non-ionic solvent (1,2,4-trichlorobenzene, TCB, Supplementary Fig. 2).

We next demonstrate the highest achieved rectification ratios in single-molecule junctions by performing I–V measurements on TDO5 (Fig. 1a) in PC. Thousands of individual I–Vs were obtained, and only traces containing a molecular feature that sustained the entire voltage ramp were considered (typically ~500–1,000 traces per molecule, see Methods). These traces were then overlaid and compiled into a two-dimensional current versus voltage histogram (Fig. 1c). The plot illustrates a clear asymmetry in current with bias sign, showing a much higher current (flowing from tip to substrate) at negative voltages than at positive voltages (tip relative to substrate). Results from analogous I–V measurements in TCB, where no asymmetry is observed, are shown in Fig. 1d.

To obtain a quantitative value for the rectification ratio (I_{on}/I_{off}), each vertical slice of the two-dimensional histogram was fit with a Gaussian, and a most probable current value was determined at each voltage to obtain an average I–V curve (overlays in Fig. 1c,d). In PC, a rectification ratio for TDO5 greater than 200 at ±370 mV is observed. Although this 'average' rectification ratio is already the highest reported for single-molecule junctions, several single-trace plots of these junctions display exceptionally high rectifying behaviour, in excess of 500, as shown in the inset of Fig. 1c. Although high rectification ratios have been observed in systems consisting of many-molecule junctions[17,18], the number of molecules involved in transport is generally unknown in these systems. Moreover, past reports have relied on asymmetric molecules, electrodes and chemical linker groups, unlike the design described here.

We hypothesize that the highly asymmetric nature of the I–V curves is due to the formation of an asymmetric, bias-dependent electric double layer. We note that a polar ion-soluble solvent is essential to observing rectification (Supplementary Fig. 3). Indeed, measurements in PC with an added electrolyte (Supplementary Fig. 4) do not differ significantly from those shown in Fig. 1. The only source of asymmetry in our experiment is the disparate areas of the two electrodes exposed to the solvent. Because molecular junctions are formed after rupturing a gold–gold contact with a

[1]Department of Applied Physics and Applied Mathematics, New York, New York 10027, USA. [2]Department of Chemistry, Columbia University, New York, New York 10027, USA. [3]Molecular Foundry, Lawrence Berkeley National Laboratory, Department of Physics, University of California, Berkeley, California 94720, USA. [4]Kavli Energy NanoSciences Institute at Berkeley, Berkeley, California 94720, USA. *e-mail: jbneaton@lbl.gov; lcampos@columbia.edu; lv2117@columbia.edu

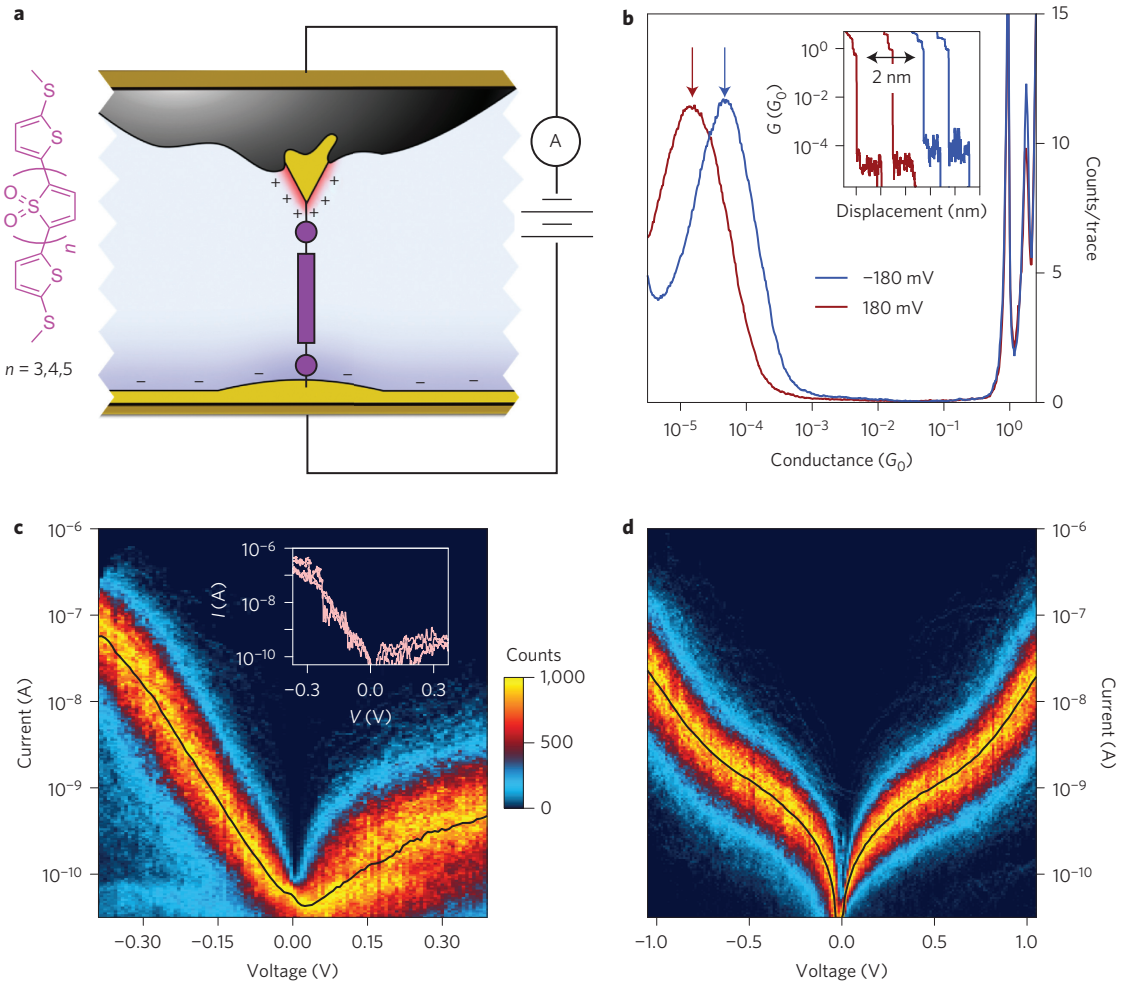

Figure 1 | Environmentally enabled single-molecule diodes. a, TDO*n* molecular structure (alkyl side chains omitted for clarity) and schematic of the molecular junction created using asymmetric area electrodes (not drawn to scale). **b**, Log-binned conductance histograms for TDO4 taken at –180 mV and +180 mV, created using 3,000 traces each and 100 bins/decade. Arrows indicate the most probably measured conductance at each bias. Inset: Sample conductance versus displacement traces, laterally offset for clarity. **c**, Two-dimensional absolute current versus voltage histogram for TDO5 in PC. Inset: Examples of exceptionally rectifying junctions (three selected traces). **d**, Two-dimensional absolute current versus voltage histogram for TDO5 in TCB. Average *I*–*V*s for TDO5 are overlaid on **c** and **d** in black.

conductance greater than $5G_0$, with electrodes of the same metal and symmetric molecules, the metal–molecule–metal structure at the nanometre scale must, on average, be completely symmetric. We therefore postulate that electric double layers at the tip and substrate, formed when ions dissolved in the polar solvent[19] move to screen out the electric field due to charges on the metal, influence the electrostatic environment around the junction. Specifically, the asymmetry in the electrode areas exposed to the solvent results in the formation of a denser double layer on the tip electrode when compared with the substrate[20]. Experimental evidence for the existence of a dense double layer around the tip can be obtained from a cyclic voltammogram of ferrocene dissolved in PC measured using the same tip/substrate system used for the rectification measurements. As shown in Supplementary Fig. 5, a clear, reversible ferrocene oxidation peak is observed at positive tip voltages, providing definitive proof that the oxidation process occurs at the tip.

To understand the rectification in these junctions in more detail, we considered a Landauer-like expression for current, assuming coherent off-resonant tunnelling through the junction, a non-interacting mean-field picture and zero temperature:

$$I = \frac{2e}{h}\int_{-eV/2}^{eV/2}\mathcal{T}(E,\varepsilon,\Gamma)\,\mathrm{d}E \qquad (1)$$

Here, e is the fundamental unit of charge, h is Planck's constant, V is the applied voltage and $\mathcal{T}(E, \varepsilon, \Gamma)$ is the energy-dependent (E) transmission function for the junction. Transmission is modelled here with a single Lorentzian peaked at the orbital energy ε and with a width Γ as[21]

$$\mathcal{T}(E,\varepsilon,\Gamma) = \frac{(\Gamma^2/4)}{(E-\varepsilon)^2 + (\Gamma^2/4)} \qquad (2)$$

Despite a clear asymmetry in $\mathcal{T}(E, \varepsilon, \Gamma)$ about the junction Fermi energy ($E = E_F$), for a symmetric junction the current, evaluated through equation (1), will be independent of the bias polarity.

We hypothesize that the double layer causes a bias polarity-dependent shift of the molecular resonance energy within the junction, leading to rectification. This bias-dependent environmental asymmetry can be modelled by replacing the resonance energy ε in equation (2) with $(\varepsilon + \alpha eV)$. Parameter α describes the impact of the applied voltage on the resonance position analogous to a first-order Stark shift coefficient. Figure 2 illustrates this model with a series of energy level diagrams where we assume, for simplicity, that $\alpha = 0.5$. At zero bias (Fig. 2a), the resonance is located at an energy ε relative to both the tip and the substrate chemical potential. When a negative voltage V is applied to the tip relative to the

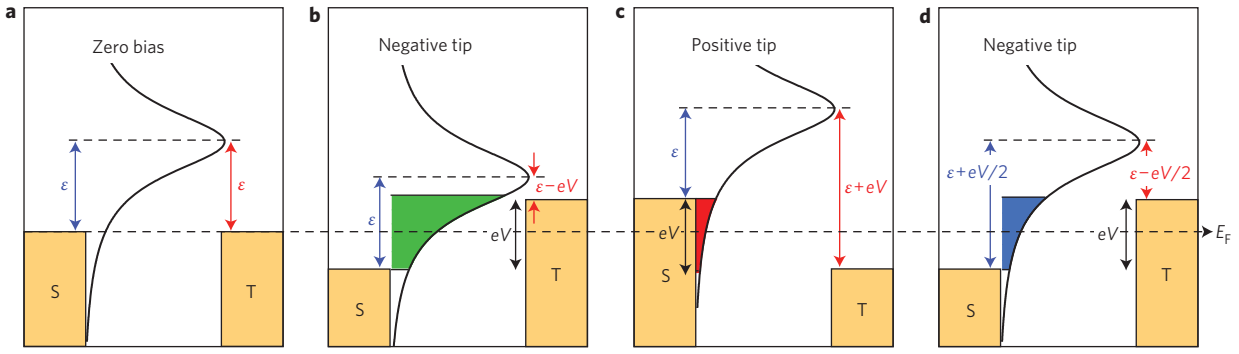

Figure 2 | Energy level diagram illustrating the rectification mechanism for a LUMO conducting molecular junction. a, Zero-bias schematic depicting a molecular resonance with peak energy ε relative to the tip (T) and substrate (S) Fermi levels E_F. **b**, In polar media, when the tip is biased negatively relative to the substrate, the molecular resonance is at $\varepsilon - eV$ relative to the tip chemical potential and at ε relative to the substrate chemical potential (here, α is taken to be 0.5). For this system, a large area (shaded green) of the resonance falls within the bias window and the current is high. **c**, When the tip is biased positively relative to the substrate, the molecular resonance again remains pinned to the substrate chemical potential, but is at $\varepsilon + eV$ relative to the tip chemical potential. A small area (shaded red) of the resonance falls within the bias window and the current is low. **d**, A similar schematic illustrating level alignment in a nonpolar solvent ($\alpha = 0$) with the tip biased negatively relative to the substrate. Here, the resonance does not shift in response to the applied bias, while both tip and substrate chemical potentials shift relative to the resonance position. The area under the resonance that falls within the bias window is independent of the bias polarity.

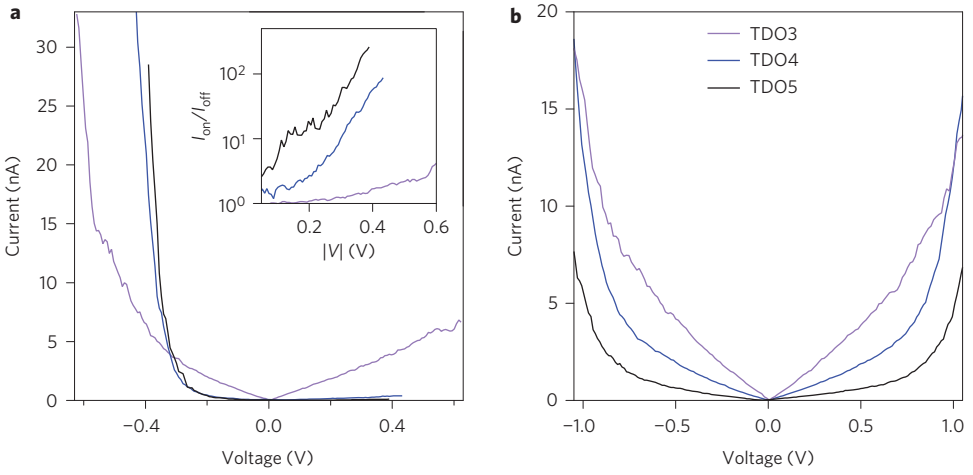

Figure 3 | High rectification ratios in TDO*n* junctions. a, Average *I*–*V*s for TDO*n* (with $n = 3$–5) measured in PC. See Supplementary Figs 6 and 7 for two-dimensional *I*–*V* maps. Inset: Rectification ratio (I_{on}/I_{off}) versus magnitude of applied voltage for *I*–*V* curves, showing ratios of ~4 at 0.6 V for TDO3, ~90 at 0.42 V for TDO4 and ~200 at 0.37 V for TDO5. We also note that the junctions rupture when the bias is increased beyond a molecule-dependent critical voltage (−0.65 V for TDO3, −0.42 V for TDO4 and −0.39 V for TDO5). We hypothesize that the LUMO resonance is at or very close to the bias window limit at this critical voltage. This would imply that we are significantly charging the molecule and potentially breaking the linker–Au donor–acceptor bonds to the electrodes. **b**, Average *I*–*V*s for TDO3–5 measured in TCB. Note that the *I*–*V* curves show the absolute value of current, for clarity. Junctions formed in TCB are typically able to withstand twice the voltage of those in PC, becoming unstable and rupturing beyond 1.1 V.

substrate, the bias window will open symmetrically, consistent with a locally symmetric junction. However, due to the tip–substrate asymmetry of the double layer, we hypothesize that the resonance shifts by an amount equal to αeV towards the tip chemical potential (Fig. 2b). When the tip is biased positively, the resonance shifts by the same amount, but in the opposite direction (Fig. 2c). We stress that, under either bias polarity, the resonance position does not change relative to the substrate chemical potential, but only relative to the tip chemical potential (when $\alpha = 0.5$). As long as $T(E, \varepsilon, \Gamma)$ is asymmetric about E_F, the current, indicated by the shaded areas in Fig. 2b,c, depends on the bias polarity yielding rectification. Figure 2d presents a non-rectifying case in solvents such as TCB, where the resonance position does not move relative to the junction E_F.

The mechanism described above implies the observation of several additional phenomena. First, rectification ratios should in general be higher for junctions composed of molecules with a sharp resonance positioned closer to E_F. Second, the molecular orbital energy closest to E_F should generally dictate the direction of rectification: highest occupied molecular orbital (HOMO)-dominated junctions should turn 'on' at the bias polarity that turns 'off' lowest unoccupied molecular orbital (LUMO)-dominated molecules. Junctions with resonances with large Γ and/or ε should yield little or no rectification, as the transmission function about E_F will be relatively flat within accessible bias windows. Finally, this rectification should occur in any polar/ionic environment.

Figure 3a presents *I*–*V* measurements for a family of derivatives containing 3–5 TDO units (TDO3–TDO5) measured in PC. For junctions in this series it has been shown previously that the LUMO moves closer to E_F with the addition of TDO units[13]. We find that all three *I*–*V* curves display strong asymmetries, with significantly more current (reaching close to 0.1 μA) at negative tip

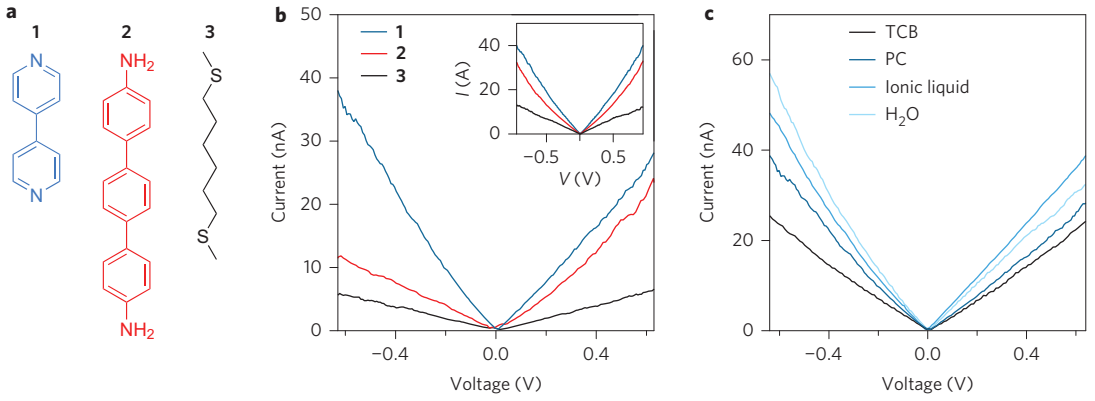

Figure 4 | Rectification with other molecule/solvent systems. a, Molecular structures of additional molecules: 4,4′-bipyridine (**1**), 4-4″-diamino-*p*-terphenyl (**2**) and 2,9-dithiadecane (**3**). **b**, *I*–*V* curves for the three molecules measured in PC and in TCB (inset). Rectification ratios of 1.4 and 2.1 are seen for **1** and **2** at 0.62 V, but **3** does not show any discernable rectification. See Supplementary Fig. 8 for corresponding two-dimensional *I*–*V* plots. **c**, *I*–*V* curves measured for **1** in TCB, PC, an ionic liquid (*N*,*N*-diethyl-*N*-(2-methoxyethyl)-*N*-methylammonium bis-(trifluoro-methylsulphonyl-imide), DEME-TFSI) and deionized water (18 MΩ). Asymmetry, and therefore rectification, is observed in these averaged *I*–*V* curves only in the polar media, and a symmetric averaged *I*–*V* curve is measured in TCB. See Supplementary Fig. 9 for corresponding two-dimensional *I*–*V* plots. Slightly different currents (and therefore rectification ratios) are observed in the various solvents. This is attributed to a solvent effect[27], whereby the work functions of the electrodes are altered by the presence of different solvent molecules adsorbed on the surface. Note that the *I*–*V* curves show the absolute value of the current, for clarity.

bias for TDO5. For all molecules, under positive tip bias (relative to the substrate) the *I*–*V* curves exhibit a more linear dependence of current on voltage, indicative of a rather flat transmission in this bias range, while the negative bias portions display a highly nonlinear behaviour (particularly for TDO4 and TDO5) that is indicative of a resonance approaching closer to the bias range.

The rectification ratios for each molecule as a function of the magnitude of the applied voltage are presented in the inset to Fig. 3a, which shows ratios of ~4 at 0.6 V for TDO3, ~90 at 0.42 V for TDO4 and ~200 at 0.37 V for TDO5. We again emphasize that these high rectification ratios occur at exceptionally low voltages. The analogous *I*–*V* measurements carried out in TCB are presented in Fig. 3b, which shows symmetric *I*–*V* curves that become increasingly nonlinear at high voltages. Evaluating these data, we confirm our first prediction: as E_F aligns closer to a molecular resonance, the rectification ratio at a given bias increases.

The impact of the dominant transport orbital on the orientation of the diode is considered next. *I*–*V* measurements were performed on three molecules that do not belong to the TDO family (Fig. 4a): 4,4′-bipyridine (**1**), 4-4″-diamino-*p*-terphenyl (**2**) and 2,9-dithiadecane (**3**). The characteristic *I*–*V*s for these measured in PC are shown in Fig. 4b. It is clear that **1** and **2** display 'on' behaviour at opposite bias polarities, while **3** does not show any discernable rectification. Within our model, this suggests that the two molecules should have transport dominated by different orbitals. Indeed, past work has shown that **1** conducts through the LUMO[22], whereas **2** conducts through the HOMO[23]. The low rectification ratios observed for **1** and **2** further suggest that the dominant transport orbitals are rather far from E_F. The large-gap alkane, **3**, does not rectify, indicating a flat transmission around E_F.

Figure 4c compares measurements of **1** in different polar media and in TCB[24]. The *I*–*V*s measured in polar media are asymmetric, with 'on' currents occurring at negative tip bias polarities. These results show clearly that our method of creating a molecular rectifier is not unique to either the TDO family or to PC as a solvent; a single-molecule diode can be created out of any molecule in any polar solvent (as long as the junction transmission function is asymmetric about E_F). All experimental results presented here support our hypothesis that a bias-dependent double layer around the tip modifies the electrostatic environment at the junction to alter the relative alignment of the molecular orbital and the tip chemical potential.

After confirming the predictions implicit in our model, we now demonstrate that we can determine the parameter α to provide quantitative support for the rectification mechanism proposed here. We used a recently developed a.c. technique[25], described briefly in the Methods and in Supplementary Section II, to determine the location of the conducting orbital (ε) and its coupling (Γ) to the Au electrodes for TDO4 in PC and TCB. The values obtained were then checked against zero-bias self-energy corrected density functional theory (DFT + Σ) calculations[23,26]. Figure 5a,b shows that, on average, ε_{TCB} is 0.6 eV, while the coupling, Γ_{TCB}, is 7 meV. The small value of Γ_{TCB} suggests that a mean-field approximation may be less adequate, particularly as the molecule charges under bias. However, departures from this picture would not be expected to alter the rectification mechanism described here. In PC we solved these two equations by allowing α to vary from 0 to 0.5 in steps of 0.05. For each value of α we obtained the average value of Γ_{PC} and ε_{PC}. Note that the coupling of the LUMO to the leads should not be altered in different solvent environments as it primarily depends on the Au density of states, which is nearly flat in the relevant energy window. Based on the results from these a.c. measurements, we find that the average Γ_{PC} is the same as Γ_{TCB} when $\alpha = 0.5$. Furthermore, we find that there is a 0.2 eV shift in ε_{PC} towards E_F compared with ε_{TCB}, which we attribute to a solvent-induced shift[27]. Using these experimentally determined ε and Γ parameters, we generated *I*–*V*s from Lorentzian transmission functions and compared these to experimentally measured *I*–*V* curves (Supplementary Fig. 10). We find reasonable agreement with the measured *I*–*V*s and rectification ratios. This simple Lorentzian model also enables us to derive an analytic form for the observed rectification ratios, which are in good agreement with the experiment (for a discussion see Supplementary Section II and Supplementary Fig. 11).

We now turn to DFT + Σ calculations to validate three features of our measurements: (1) the transmission function for TDO4 is well described by a Lorentzian function; (2) PC alters the level alignment in the junction but not the coupling; and (3) adding a dipole layer on one electrode shifts the resonance position. We show the calculated zero-bias transmission functions for a TDO4 junction with and without PC (structures shown in Fig. 5c) in Fig. 5d. We find that these transmission curves are well described by a single Lorentzian form dominated by the LUMO, that these have a

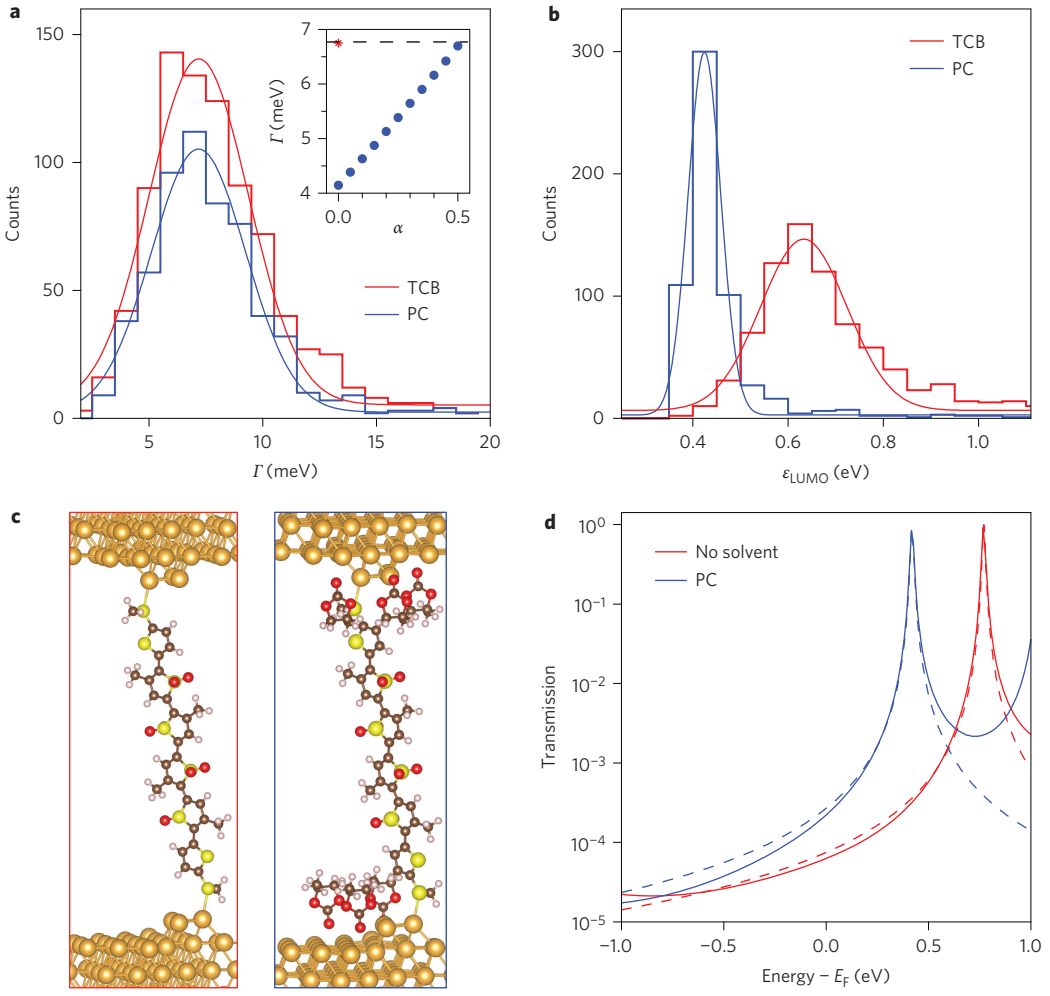

Figure 5 | Experimental and computational determination of energy level alignment. a,**b**, Experimental determination of orbital coupling strength (**a**) and energy level alignment (**b**) for TDO4 in TCB and PC, determined using a.c. techniques. Inset in **a**: Orbital coupling as a function of bias asymmetry parameter α. The average value of the coupling for TCB junctions (red asterisk) is only achieved for $\alpha = 0.5$, which corresponds to a resonance that is pinned to the substrate chemical potential. The dashed line is shown to guide the eye to make the comparison more apparent. **c**, Junction structures used to compute transmission functions. **d**, DFT + Σ calculated transmission functions for TDO4 in a junction with no solvent molecules (red) and with PC on both electrodes (blue). Dashed lines indicate Lorentzian fits to these transmission functions. These fits yield identical coupling strengths for the conducting orbital ($\Gamma = 13$ meV) for both junctions, and show a decrease in orbital position relative to E_F when adding PC around the junction ($\varepsilon = 440$ meV, blue; $\varepsilon = 760$ meV, red).

similar Γ, and that they show a relative shift in ε of ~0.3 eV. To model a dipole layer on one electrode we added a layer of HF molecules within the unit cell oriented with the dipole pointing towards or away from the electrode, and computed transmission through the TDO4 junction. Results from these calculations are shown in Supplementary Fig. 12. The presence of a dipole oriented with the negative charge close to the electrode shifts the resonance position closer to E_F. We stress here that these are zero-bias calculations and, as such, cannot be used to quantitatively address the shift in the resonance position due to an applied bias as this depends on the double layer density. A first-principles determination of α would require computing the impact of the double layer around the tip on the resonance position and is beyond the scope of this work.

Although we do not have an atomistic model for the observed rectification effects, the results from the a.c. measurements and the DFT + Σ calculations support our postulated mechanism. To summarize, two factors are needed to observe rectification: (1) electrodes of different areas and (2) an ion-containing polar medium in which the transport measurements are performed. Due to the presence of ions in the environment, an electric double layer forms at each electrode/solution interface to screen out any applied bias. The disparate areas of the electrodes result in a denser layer of charge at the smaller tip electrode. This results in the pinning of the molecular orbitals to the chemical potential of the substrate, yielding a current dependence on the polarity of the applied bias.

We have demonstrated an unconventional technique with which to create single-molecule diodes with unprecedented rectification ratios at low operating voltages using symmetric molecules. This appealing and simple method enables the creation of single-molecule junctions by self-assembly, without the tedious chemical modifications that have commonly been used to control molecule directionality in a junction[7]. Given the observed mechanism of rectification, we envisage that this method can be easily implemented in other junctions beyond the STM-BJ test bed. For example, the use of other electrode materials including carbon nanotubes[28] or graphene[29] should yield rectifying behaviour. By exploiting this tunable asymmetry in the electrostatic environment, this new approach offers a wealth of possibilities for translation into device fabrication.

Methods

Methods and any associated references are available in the online version of the paper.

Received 3 November 2014; accepted 14 April 2015; published online 25 May 2015

References

1. Nitzan, A. & Ratner, M. A. Electron transport in molecular wire junctions. *Science* **300,** 1384–1389 (2003).
2. Tao, N. J. Electron transport in molecular junctions. *Nature Nanotech.* **1,** 173–181 (2006).
3. Aradhya, S. V. & Venkataraman, L. Single-molecule junctions beyond electronic transport. *Nature Nanotech.* **8,** 399–410 (2013).
4. Ellenbogen, J. C. & Love, J. C. Architectures for molecular electronic computers. I. Logic structures and an adder designed from molecular electronic diodes. *Proc. IEEE* **88,** 386–426 (2000).
5. Aviram, A. & Ratner, M. A. Molecular rectifiers. *Chem. Phys. Lett.* **29,** 277–283 (1974).
6. Mayor, M. *et al.* Electric current through a molecular rod—relevance of the position of the anchor groups. *Angew. Chem. Int. Ed.* **42,** 5834–5838 (2003).
7. Diez-Perez, I. *et al.* Rectification and stability of a single molecular diode with controlled orientation. *Nature Chem.* **1,** 635–641 (2009).
8. Lortscher, E. *et al.* Transport properties of a single-molecule diode. *ACS Nano* **6,** 4931–4939 (2012).
9. Batra, A. *et al.* Tuning rectification in single-molecular diodes. *Nano Lett.* **13,** 6233–6237 (2013).
10. Kim, T., Liu, Z. F., Lee, C., Neaton, J. B. & Venkataraman, L. Charge transport and rectification in molecular junctions formed with carbon-based electrodes. *Proc. Natl Acad. Sci. USA* **111,** 10928–10932 (2014).
11. Elbing, M. *et al.* A single-molecule diode. *Proc. Natl Acad. Sci. USA* **102,** 8815–8820 (2005).
12. Stokbro, K., Taylor, J. & Brandbyge, M. Do Aviram–Ratner diodes rectify? *J. Am. Chem. Soc.* **125,** 3674–3675 (2003).
13. Dell, E. J., Capozzi, B., Xia, J., Venkataraman, L. & Campos, L. M. Molecular length dictates the nature of charge carriers in single-molecule junctions of oxidized oligothiophenes. *Nature Chem.* **7,** 209–214 (2015).
14. Barbarella, G., Pudova, O., Arbizzani, C., Mastragostino, M. & Bongini, A. Oligothiophene-*S*,*S*-dioxides: a new class of thiophene-based materials. *J. Org. Chem.* **63,** 1742–1745 (1998).
15. Xu, B. Q. & Tao, N. J. Measurement of single-molecule resistance by repeated formation of molecular junctions. *Science* **301,** 1221–1223 (2003).
16. Nagahara, L. A., Thundat, T. & Lindsay, S. M. Preparation and characterization of STM tips for electrochemical studies. *Rev. Sci. Instrum.* **60,** 3128–3130 (1989).
17. Metzger, R. M. Unimolecular electrical rectifiers. *Chem. Rev.* **103,** 3803–3834 (2003).
18. Nerngchamnong, N. *et al.* The role of van der Waals forces in the performance of molecular diodes. *Nature Nanotech.* **8,** 113–118 (2013).
19. Ciszkowska, M. & Stojek, Z. Voltammetry in solutions of low ionic strength. Electrochemical and analytical aspects. *J. Electroanal. Chem.* **466,** 129–143 (1999).
20. Bard, A. J. & Faulkner, L. R. *Electrochemical Methods: Theory and Applications* (Wiley, 2001).
21. Paulsson, M. & Datta, S. Thermoelectric effect in molecular electronics. *Phys. Rev. B* **67,** 241403 (2003).
22. Quek, S. Y. *et al.* Mechanically controlled binary conductance switching of a single-molecule junction. *Nature Nanotech.* **4,** 230–234 (2009).
23. Quek, S. Y. *et al.* Amine–gold linked single-molecule circuits: experiment and theory. *Nano Lett.* **7,** 3477–3482 (2007).
24. Darancet, P., Widawsky, J. R., Choi, H. J., Venkataraman, L. & Neaton, J. B. Quantitative current–voltage characteristics in molecular junctions from first principles. *Nano Lett.* **12,** 6250–6254 (2012).
25. Adak, O., Korytar, R., Joe, A. Y., Evers, F. & Venkataraman, L. Impact of electrode density of states on transport through pyridine-linked single molecule junctions. Preprint at http://arXiv.org/abs/1504.00242 (2015).
26. Brandbyge, M., Mozos, J. L., Ordejon, P., Taylor, J. & Stokbro, K. Density-functional method for nonequilibrium electron transport. *Phys. Rev. B* **65,** 165401 (2002).
27. Fatemi, V., Kamenetska, M., Neaton, J. B. & Venkataraman, L. Environmental control of single-molecule junction transport. *Nano Lett.* **11,** 1988–1992 (2011).
28. Guo, X. F. *et al.* Covalently bridging gaps in single-walled carbon nanotubes with conducting molecules. *Science* **311,** 356–359 (2006).
29. Prins, F. *et al.* Room-temperature gating of molecular junctions using few-layer graphene nanogap electrodes. *Nano Lett.* **11,** 4607–4611 (2011).

Acknowledgements

The authors thank M. Hybertsen and M. Steigerwald for discussions. The experimental work was supported primarily by the National Science Foundation (award no. DMR-1206202). E.J.D. acknowledges the HHMI, the American Australian Association and Dow Chemical Company for International Research Fellowships. The computational work was supported by the Molecular Foundry, and by the Materials Sciences and Engineering Division (Theory FWP), US Department of Energy, Office of Basic Energy Sciences (contract no. DE-AC02-05CH11231). Portions of the computation work were performed at National Energy Research Scientific Computing Center. O.A. acknowledges support from the NSF (award no. DMR-1122594). L.V. thanks the Packard Foundation for support.

Author contributions

Experiments were conceived and designed by B.C., O.A., L.M.C., J.B.N. and L.V. and performed by B.C., O.A. and J.C.T. Data analysis was carried out by B.C. and O.A. Compounds were synthesized by J.L. and E.J.D. Calculations were performed by Z-F.L. and J.B.N. The manuscript was co-written by B.C., J.B.N., L.M.C. and L.V., with input from all authors.

Additional information

Supplementary information is available in the online version of the paper. Reprints and permissions information is available online at www.nature.com/reprints. Correspondence and requests for materials should be addressed to J.B.N., L.M.C. and L.V.

Competing financial interests

The authors declare no competing financial interests.

Methods

Conductance measurements. Conductance measurements were carried out using the STM-BJ technique[15] and have been described in detail elsewhere[30]. Conductance measurements for the TDO*n* family (for synthetic details see Supplementary Section IV and Supplementary Fig. 13) were carried out in dilute solutions (10–100 μM) in PC and TCB. Measurements for all other molecules (obtained from commercial sources, with over 95% purity) were carried out from 1 mM concentration solutions. The insulated tips were created by driving a mechanically cut gold tip through Apiezon wax[16]. One-dimensional conductance histograms were constructed using logarithmic bins (100 per decade) without any data selection.

Current–voltage measurements. *I*–*V* measurements were performed using the STM-BJ technique, with a slightly modified procedure[31]. Instead of continuously retracting the tip from the substrate, the tip was withdrawn for 150 ms, held for 150 ms, and then withdrawn for an additional 200 ms to fully rupture the molecular junction. A constant voltage was applied during the initial and final segments, as well as during the first and last 25 ms when the tip position was held fixed. During the central 100 ms during which the tip was held, a voltage ramp was applied. Current was measured during the entire 500 ms procedure (for a sample trace see Supplementary Fig. 1). *I*–*V* data were analysed by first selecting traces with a molecular junction that sustained the entirety of the voltage ramp. Traces were selected using an automated algorithm that required the conductance during the first and last 25 ms of the hold to be within the width of the molecular conductance histogram. *I*–*V*s in TCB were collected over a range of ±1.05 V, while *I*–*V*s in PC were collected over smaller molecule-dependent voltage ranges. After trace selection, all *I*–*V*s for a given molecule were used to construct a two-dimensional current versus voltage histogram. A most probable *I*–*V* was obtained by fitting each vertical line slice of the two-dimensional *I*–*V* histogram with a Gaussian and recording the peak current. This was then converted to its linearly scaled *I*–*V* curve following the procedure detailed by Huber and co-authors[32].

Alternating-current measurement technique. The differential conductance ($G = \mathrm{d}I/\mathrm{d}V$) and derivative of conductance with respect to voltage ($\mathrm{d}G/\mathrm{d}V$) were measured simultaneously while applying a d.c. and an a.c. voltage across the junctions in both PC and TCB. Analytical expressions for these quantities in terms of orbital energy level alignment and molecular coupling strength were next obtained assuming a single Lorentzian transmission, which was justified by the DFT calculations. We included the effect of bias voltage on ε, as detailed in the main text, through parameter α. For the TCB case, the set of two nonlinear equations was solved for Γ and ε with $\alpha = 0$; that is, the LUMO position was unaltered by the applied bias.

Computational details. To compute the transport properties of the molecular junctions, an *ab initio* approach was used based on a combination of DFT, non-equilibrium Green's functions (NEGFs)[26] and a GW-based self-energy correction[33], DFT + Σ[23]. To reduce the computational cost, we replaced the long $-C_6H_{13}$ chains in the molecules by $-CH_3$. The molecules were placed between two gold leads consisting of seven Au (111) layers on each side, with 16 (4 × 4) atoms on each layer, to form molecular junctions. Due to the donor–acceptor nature of the Au–S bond, we used trimers as the binding motif, consistent with previous work[23]. The junction geometry was relaxed using the Perdew–Burke–Ernzerhof (PBE)[34] functional implemented in SIESTA. The Au basis set and pseudopotential were adapted from previous work[23]. The outer three layers of gold atoms were fixed in their bulk geometry during relaxation. A 4 × 4 k-mesh was used and the atomic coordinates were relaxed until all forces were below 0.04 eV $Å^{-1}$. The resulting Au–S bond lengths were ~2.85 Å, and the angle between the Au–S bond and the thiophene plane was ~20°. After the junction geometry was relaxed, the transport properties were computed using the DFT-NEGF formalism as implemented in TranSIESTA[26]. The outer three layers of gold atoms formed the leads, and the extended molecule consisted of four gold layers on each side. The PBE functional, a 6 × 6 k-mesh and 36 energy grid points in the integration contour were used[26] to converge the non-equilibrium density matrix. Due to the inaccuracy of PBE level alignment between the junction Fermi level and molecular frontier orbital energies[33], we used a self-energy correction to the PBE Kohn–Sham Hamiltonian in the non-self-consistent calculation of transmission function $T(E)$, as detailed in the Supplementary Section III.

References

30. Venkataraman, L., Klare, J. E., Nuckolls, C., Hybertsen, M. S. & Steigerwald, M. L. Dependence of single-molecule junction conductance on molecular conformation. *Nature* **442,** 904–907 (2006).
31. Widawsky, J. R. *et al.* Measurement of voltage-dependent electronic transport across amine-linked single-molecular-wire junctions. *Nanotechnology* **20,** 434009 (2009).
32. Huber, R. *et al.* Electrical conductance of conjugated oligormers at the single molecule level. *J. Am. Chem. Soc.* **130,** 1080–1084 (2008).
33. Neaton, J. B., Hybertsen, M. S. & Louie, S. G. Renormalization of molecular electronic levels at metal–molecule interfaces. *Phys. Rev. Lett.* **97,** 216405 (2006).
34. Perdew, J. P., Burke, K. & Ernzerhof, M. Generalized gradient approximation made simple. *Phys. Rev. Lett.* **77,** 3865–3868 (1996).